



Research articles

Spin-flop phase transition in the orthorhombic antiferromagnetic topological semimetal $\text{Cu}_{0.95}\text{MnAs}$ Eve Emmanouilidou^a, Jinyu Liu^a, David Graf^b, Huibo Cao^c, Ni Ni^{a,*}^a Department of Physics and Astronomy, University of California, Los Angeles, CA 90095, USA^b National High Magnetic Field Laboratory, 1800 E. Paul Dirac Drive, Tallahassee, FL 32310, USA^c Quantum Condensed Matter Division, Oak Ridge National Laboratory, Oak Ridge, TN 37831, USA

ARTICLE INFO

Keywords:

Metamagnetism
Spin flop transition
Topological semimetal

ABSTRACT

The orthorhombic antiferromagnetic compound CuMnAs was recently predicted to be an antiferromagnetic Dirac semimetal if both the R_y gliding and the S_{2z} rotational symmetries are preserved in its magnetic ordered state. In our previous work on $\text{Cu}_{0.95}\text{MnAs}$ and $\text{Cu}_{0.98}\text{Mn}_{0.96}\text{As}$, we showed that in their low temperature commensurate antiferromagnetic state the b -axis is the magnetic easy axis, breaking the S_{2z} symmetry and resulting in a polarized surface state that could make this material potentially interesting for antiferromagnetic spintronics. In this paper, we report a detailed study of the anisotropic magnetic properties and magnetoresistance of $\text{Cu}_{0.95}\text{MnAs}$ and $\text{Cu}_{0.98}\text{Mn}_{0.96}\text{As}$. Our study shows that in $\text{Cu}_{0.95}\text{MnAs}$ the magnetic easy axis is along the b direction and the hard axis is along c . Furthermore, it reveals that $\text{Cu}_{0.95}\text{MnAs}$ features a spin-flop phase transition at high temperatures and low fields when the field is applied along the easy b axis. However, no metamagnetic transition is observed for $\text{Cu}_{0.98}\text{Mn}_{0.96}\text{As}$, indicating that the magnetic interactions in this system are very sensitive to Cu vacancies and Cu/Mn site mixing.

1. Introduction

Antiferromagnetic (AFM) materials have recently brought new excitement to the field of condensed matter physics due to their potential applications in spintronics, a field which studies the effect of the charge carrier spin in conduction. AFM systems lack a net magnetic moment although the individual atoms are magnetic, and this makes them “invisible” to external magnetic fields, which originally led researchers to believe that they could not be used for practical applications [1]. It was not until a few years ago that it was realized that antiferromagnets have many characteristics that make them suitable for spintronics; they are insensitive to magnetic field perturbations, do not generate stray fields, and have faster spin dynamics than ferromagnets since their resonant frequencies are higher [1,2]. The prediction and subsequent discovery of the anomalous Hall effect [3,4] and the spin Hall effect [5–7] in AFMs have also contributed to their recent popularity.

Tetragonal CuMnAs has been studied for its potential applicability as an AFM spintronic material since 2013 [8,9]. Recently, its orthorhombic polymorph was proposed to host Dirac fermions [10]. If the combination of inversion and time-reversal symmetries, \mathcal{PT} , is preserved, the existence of Dirac fermions can be achieved when both the R_y gliding and the S_{2z} rotational symmetries are preserved in the

magnetic state. The Dirac fermions in CuMnAs have also been predicted to be controlled by the spin-orbit torque reorientation of the Néel vector [11].

In our previous paper, we first reported on the synthesis and magnetic structures of single crystalline $\text{Cu}_{0.95}\text{MnAs}$, which crystallizes in the $Pnma$ space group with lattice parameters $a = 6.5716(4) \text{ \AA}$, $b = 3.8605(2) \text{ \AA}$, and $c = 7.3047(4) \text{ \AA}$, and $\text{Cu}_{0.98}\text{Mn}_{0.96}\text{As}$, with lattice parameters $a = 6.5868(4) \text{ \AA}$, $b = 3.8542(3) \text{ \AA}$, and $c = 7.3015(5) \text{ \AA}$ [12]. Although an additional intermediate incommensurate AFM state exists in $\text{Cu}_{0.98}\text{Mn}_{0.96}\text{As}$, when both $\text{Cu}_{0.95}\text{MnAs}$ and $\text{Cu}_{0.98}\text{Mn}_{0.96}\text{As}$ are in their low-temperature commensurate AFM state, neutron diffraction measurements reveal that the Mn spins of the distorted Mn honeycomb sublattice order antiparallel to each of their nearest neighbors with the spins along the b -axis. We concluded that this magnetic structure breaks the S_{2z} symmetry, leading to the disappearance of Dirac fermions. This is consistent with a subsequent study of CuMnAs single crystals that found that the easy axis is in the ab plane [13]. Our first-principles calculations show that this magnetic order can support spin-polarized states, a much sought after property for spintronics.

In this paper, we discuss the observation of a metamagnetic phase transition in $\text{Cu}_{0.95}\text{MnAs}$, and its absence in $\text{Cu}_{0.98}\text{Mn}_{0.96}\text{As}$, through a thorough study of magnetic susceptibility and magnetoresistance, and

* Corresponding author.

E-mail address: nini@physics.ucla.edu (N. Ni).<https://doi.org/10.1016/j.jmmm.2018.08.084>

Received 14 May 2018; Received in revised form 30 August 2018; Accepted 30 August 2018

Available online 01 September 2018

0304-8853/ © 2018 Elsevier B.V. All rights reserved.

present a magnetic phase diagram for $\text{Cu}_{0.95}\text{MnAs}$.

2. Experimental methods

CuMnAs single crystals were synthesized using the flux method. Chunks of Bi were used as the flux, with the recipes described in detail in Refs. [12,14]. Magnetic susceptibility data with the magnetic field applied parallel to the a , b and c crystallographic axes were collected in a Quantum Design (QD) Magnetic Property Measurement System (MPMS). In order to acquire a large enough signal, four to five pieces were carefully aligned on a quartz holder that contributes very little to the magnetic signal. Electrical resistivity (ρ_{xx}) and magnetoresistance (MR) were measured in a QD Physical Property Measurement System (PPMS) under magnetic fields from -9 T to 9 T, and the National High Magnetic Field Lab (NHMFL) in Tallahassee, FL for fields up to 35 T. The MR was calculated using equation $\text{MR} = \frac{\rho_{xx}(H) - \rho_{xx}(0)}{\rho_{xx}(0)}$, after $\rho_{xx}(H)$ had been symmetrized. An excitation current of a few mA was applied parallel to the b axis in all cases.

3. Results and discussion

Fig. 1 shows the temperature dependence of the magnetic susceptibility χ of $\text{Cu}_{0.95}\text{MnAs}$ under a magnetic field of 1 T, applied parallel to the a , b and c axes. $\text{Cu}_{0.95}\text{MnAs}$ undergoes a temperature induced second-order paramagnetic (PM) to AFM phase transition at 360 K and the effect of the transition is most pronounced when $H//b$, as the susceptibility begins to decrease dramatically below this temperature. With $H//a$ and $H//c$, χ shows much smaller change across 360 K, which can be better seen in the $d(\chi T)/dT$ plot shown in the inset of Fig. 1. This suggests that the magnetic easy axis for $\text{Cu}_{0.95}\text{MnAs}$ is the b axis, which is consistent with the neutron diffraction results [12]. No Curie–Weiss behavior is observed up to 400 K.

As the sample is further cooled, a second anomaly is observed around 30 K. In contrast to the high temperature transition, the susceptibility with $H//a$ starts decreasing sharply, while increasing along the other two directions. For $H//b$ the increase is dramatic; the susceptibility at 2 K is more than twice as large as that at 30 K. This transition can also be clearly seen in the inset of Fig. 1.

To investigate the nature of this low temperature transition, we measured the isothermal magnetization of $\text{Cu}_{0.95}\text{MnAs}$ with $H//b$ from

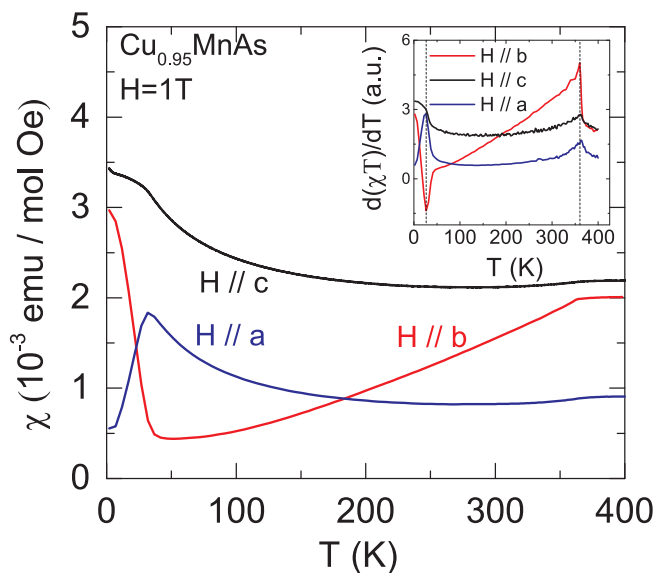


Fig. 1. Temperature dependence of the susceptibility (χ) of $\text{Cu}_{0.95}\text{MnAs}$ with a magnetic field of 1 T, applied parallel to the a , b and c crystallographic axes. Inset: The derivative of the quantity χT with respect to temperature.

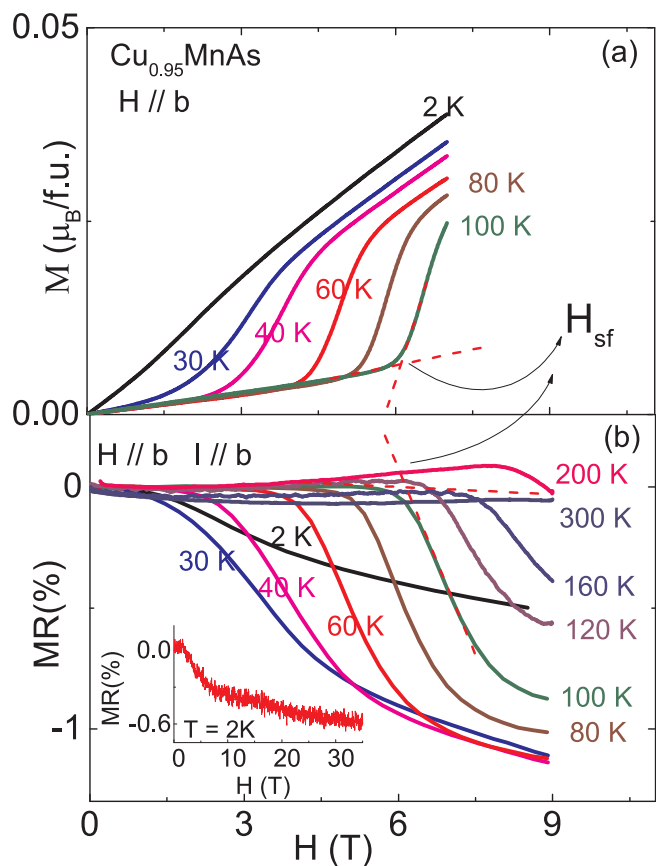


Fig. 2. (a): The magnetization, M , of $\text{Cu}_{0.95}\text{MnAs}$ at various temperatures for $H//b$. (b): The magnetoresistance, MR , of $\text{Cu}_{0.95}\text{MnAs}$ at various temperatures, for $H//b$ and $I//b$. Inset: The MR for fields up to 35 T. The criteria to determine the critical spin-flop field H_{sf} are shown in (a) and (b).

2 K to 100 K, as shown in Fig. 2(a). These field dependent magnetization curves show sharp upturns with increasing field, suggesting a spin-flop transition. This phenomenon was first experimentally observed in $\text{CuCl}_2 \cdot \text{H}_2\text{O}$ single crystals [15], and has since been observed in many other systems with magnetocrystalline anisotropy [16–24]. Spin-flop transitions can take place in materials with weak magnetocrystalline anisotropy. When a magnetic field is applied parallel to the magnetic easy axis of the material and exceeds a critical value H_{SF} , the simple staggered antiferromagnetic spins suddenly rotate into a canted spin-flop state with the spins trying to align perpendicular to the magnetic field, and this leads to a net moment along the easy axis [25]. Upon further increasing the field, the net moment grows until the spins are fully polarized and the moment saturates. The spin-flop transition occurs because the total energy of the system is a sum of the Zeeman energy of each magnetic sublattice and the magnetic anisotropy energy. At low fields the AFM configuration is the ground state, but above H_{SF} , it is the canted spin-flop state with spins almost normal to the field that minimizes the energy [26].

No hysteresis is observed in Fig. 2(a), as is the case for most AFM materials with spin-flop transitions, which can be first- or second-order. For years the spin-flop transition had been considered to be a first-order transition, with the absence of the magnetic hysteresis attributed to low magnetic anisotropy, but its nature is now being reinvestigated as it is believed that it could be second-order [27]. No saturation is observed up to 7 T for $\text{Cu}_{0.95}\text{MnAs}$, indicating that the system remains in the canted spin-flop state. This is consistent with the fact that the maximum magnetic moment at 2 K and 7 T is just $0.04 \mu_B/\text{f.u.}$, much smaller than the saturation moment of Mn^{2+} .

The spin-flop transition can also be clearly seen in the isothermal

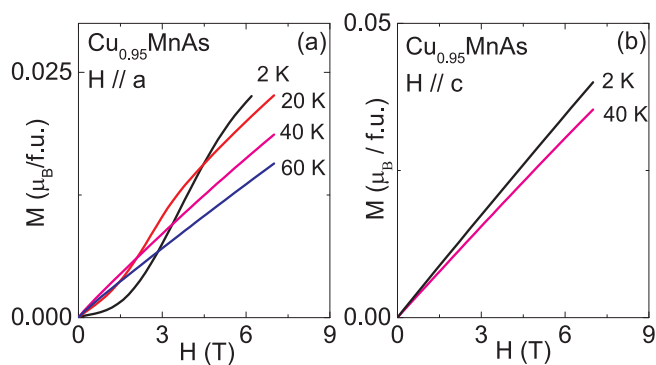


Fig. 3. (a): The field dependence of the magnetization of $\text{Cu}_{0.95}\text{MnAs}$ for 2 K, 20 K, 40 K and 60 K with the field parallel to a . (b): The field dependence of the magnetization of $\text{Cu}_{0.95}\text{MnAs}$ for 2 K and 40 K with the field parallel to c .

MR data, shown in Fig. 2(b) for temperatures from 2 K to 300 K. Associated with the transition is a sharp drop in the MR up to around -1% at 9 T, suggesting the loss of spin scattering above H_{SF} , which is consistent with the spin-flop transition scenario. The transition persists for temperatures up to 200 K and H_{SF} continues to increase, reaching $\approx 7.8\text{ T}$ at 200 K. The exact value becomes difficult to determine at higher temperatures as the drop in the MR decreases, the data become noisy due to thermal fluctuations and H_{SF} approaches 9 T, the highest field that we can apply. The inset of Fig. 2(b) shows the MR measured up to 35 T at 2 K. It decreases linearly above 9 T, suggesting that the system remains in the spin-flop state up to 35 T without saturation. The critical fields in both measurements are in very good agreement and the small mismatches can be ascribed to misalignment between the magnetic field direction and the magnetic easy axis.

To further investigate the magnetic anisotropy, we measured the isothermal magnetization of $\text{Cu}_{0.95}\text{MnAs}$ with $H//a$ and $H//c$ and the data is shown in Fig. 3(a) and (b), respectively. With $H//a$, the isothermal magnetization shows a metamagnetic transition below 30 K, while linearly increasing with field above 30 K. This is in sharp contrast to what we observe when $H//b$, where the metamagnetic transition can be observed even at 100 K. When the field is parallel to the c direction, the magnetization remains linear with field at both 2 K and 40 K up to 7 T, showing no sign of a metamagnetic transition. This behavior suggests that the magnetic easy axis is along the b direction and the hard axis is along c , consistent with the neutron scattering data [12].

A proposed magnetic phase diagram for $\text{Cu}_{0.95}\text{MnAs}$, based on our results from magnetization and magnetoresistance with the field parallel to the easy axis ($H//b$) is shown in Fig. 4. The H_{SF} at each temperature is determined from the isothermal magnetization data using the criterion shown in Fig. 2(a), where we define H_{SF} as the field at which the slope of the curve begins to change. We can apply the criterion shown in Fig. 2(b) to determine the H_{SF} from the MR data, as the MR consists of an initial plateau followed by a sharp decrease. However, we can only apply this criterion safely for temperatures above 40 K, as below this temperature it becomes difficult to distinguish between the two phases. The critical fields from the two measurements are in good agreement and the phase diagram consists of a low field AFM state with the Mn spins oriented along the b axis and a high field canted spin-flop phase with spins that have now flopped and form a canted AFM structure. Note that the critical field at 30 K is around 1.1 T, in good agreement with the magnetic susceptibility data.

In our previous study we showed that in orthorhombic CuMnAs , the magnetism is very sensitive to the Cu vacancies and Cu/Mn site mixing [12]. While $\text{Cu}_{0.95}\text{MnAs}$ is a commensurate antiferromagnet below 360 K, $\text{Cu}_{0.98}\text{Mn}_{0.96}\text{As}$ enters an incommensurate antiferromagnetic state at 320 K and then a commensurate antiferromagnetic state below 230 K. To further examine the effect of Cu vacancies and Cu/Mn site mixing on the spin-flop phase transition, we performed isothermal

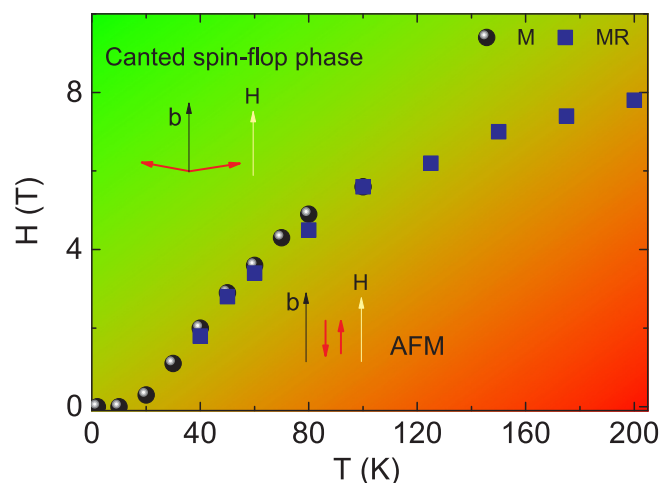


Fig. 4. The magnetic phase diagram of $\text{Cu}_{0.95}\text{MnAs}$ with the field parallel to the b axis. The black circles correspond to H_{SF} determined from magnetization measurements and the blue squares refer to H_{SF} determined from MR measurements. (For interpretation of the references to colour in this figure legend, the reader is referred to the web version of this article.)

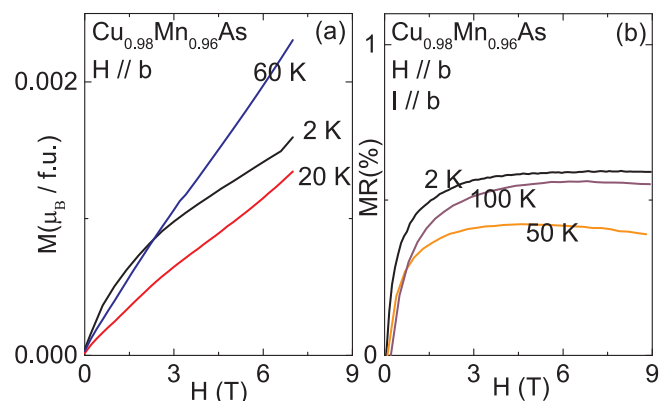


Fig. 5. (a)–(b): The isothermal magnetization (a) and magnetoresistance (b) of $\text{Cu}_{0.98}\text{Mn}_{0.96}\text{As}$ at a few different temperatures. The magnetic field was applied parallel to the b axis.

magnetization and magnetoresistance measurements on $\text{Cu}_{0.98}\text{Mn}_{0.96}\text{As}$. The data are summarized in Figs. 5(a) and (b), respectively. No sign of a spin-flop transition is observed. The field-dependent magnetization evolves from a convex shape at 2 K to linear behavior at 60 K, with no sharp upturn. The MR is positive and quickly plateaus, reaching a maximum value of 0.5%. These observations suggest that a few % of Cu vacancies or mixing with Mn atoms can destroy the spin-flop transition, confirming that the magnetism in this system is very sensitive to defects.

4. Conclusion

In conclusion, we have studied the magnetization and magnetoresistance of $\text{Cu}_{0.95}\text{MnAs}$ and $\text{Cu}_{0.98}\text{Mn}_{0.96}\text{As}$ single crystals. Both measurements confirm that $\text{Cu}_{0.95}\text{MnAs}$ undergoes a metamagnetic spin-flop transition at high temperatures and low fields with the field along the easy axis b , leading to a canted antiferromagnetic state with a small net moment along the b axis. On the other hand, in $\text{Cu}_{0.98}\text{Mn}_{0.96}\text{As}$ these transitions are absent, suggesting a dramatic effect of Cu vacancies or Cu/Mn mixing on the magnetism in the orthorhombic CuMnAs compound.

Acknowledgments

Work at UCLA was supported by the U.S. Department of Energy (DOE), Office of Science, Office of Basic Energy Sciences under Award Number DE-SC0011978 and the NSF-MRI grant 1625776. The National High Magnetic Field Laboratory is supported by the National Science Foundation through NSF/DMR-1644779 and the State of Florida.

References

- [1] T. Jungwirth, X. Marti, P. Wadley, J. Wunderlich, Antiferromagnetic spintronics, *Nat. Nanotechnol.* 11 (2016) 231.
- [2] M.B. Jungfleisch, W. Zhang, A. Hoffmann, Perspectives of antiferromagnetic spintronics, *Phys. Lett. A* 382 (2018) 865.
- [3] H. Chen, Q. Niu, A.H. MacDonald, Anomalous hall effect arising from noncollinear antiferromagnetism, *Phys. Rev. Lett.* 112 (2014) 017205.
- [4] C. Suurgers, W. Kittler, T. Wolf, H.V. Lohneysen, Anomalous Hall effect in the noncollinear antiferromagnet Mn_5Si_3 , *AIP Adv.* 6 (2016) 55604.
- [5] J.B.S. Mendes, R.O. Cunha, O. Alves Santos, P.R.T. Ribeiro, F.L.A. Machado, R.L. Rodriguez-Suarez, A. Azevedo, S.M. Rezende, Large inverse spin Hall effect in the antiferromagnetic metal $\text{Ir}_{20}\text{Mn}_{80}$, *Phys. Rev. B* 89 (2014) 140406(R).
- [6] W. Zhang, M.B. Jungfleisch, W. Jiang, J.E. Pearson, A. Hoffmann, F. Freimuth, Y. Mokrousov, Spin hall effects in metallic antiferromagnets, *Phys. Rev. Lett.* 113 (2014) 196602.
- [7] Y. Ou, S. Shi, D.C. Ralph, R.A. Buhrman, Strong spin hall effect in the antiferromagnet PtMn, *Phys. Rev. B* 93 (2016) 220405(R).
- [8] P. Wadley, V. Novak, R.P. Campion, C. Rinaldi, X. Marti, H. Reichlova, J. Zelezny, J. Gazquez, M.A. Roldan, M. Varela, et al., Tetragonal phase of epitaxial room-temperature antiferromagnet CuMnAs, *Nat. Commun.* 4 (2013) 2322.
- [9] P. Wadley, V. Hills, M.R. Shahedkhan, K.W. Edmonds, R.P. Campion, V. Novak, B. Ouladdiaf, D. Khalyavin, S. Langridge, V. Saidl, et al., Antiferromagnetic structure in tetragonal CuMnAs thin films, *Sci. Rep.* 5 (2015) 17079.
- [10] P. Tang, Q. Zhou, G. Xu, S.-C. Zhang, Dirac fermions in an antiferromagnetic semimetal *Nat. Phys.* 12 (2016) 1100.
- [11] L. Smejkal, J. Zelezny, J. Sinova, T. Jungwirth, Electric control of dirac quasi-particles by spin-orbit torque in an antiferromagnet, *Phys. Rev. Lett.* 118 (2017) 106402.
- [12] E. Emmanouilidou, H. Cao, P. Tang, X. Gui, C. Hu, B. Shen, J. Wu, S.-C. Zhang, W. Xie, N. Ni, Magnetic order induces symmetry breaking in the single-crystalline orthorhombic CuMnAs semimetal, *Phys. Rev. B* 96 (2017) 224405.
- [13] X. Zhang, S. Sun, H. Lei, Massive fermions with low mobility in antiferromagnet orthorhombic CuMnAs single crystals, *Phys. Rev. B* 96 (2017) 235105.
- [14] K. Uhlířová, R. Tarasenko, F. Javier Martínez-Casado, B. Vondracková, Z. Matěj, Synthesis and single crystal study of CuMn_3As_2 and $\text{Cu}_2\text{Mn}_4\text{As}_3$, *J. Alloys Compd.* 650 (2015) 224.
- [15] N.J. Poulis, J. van den Handel, J. Ubbink, J.A. Poulis, C.J. Gorter, On antiferromagnetism in a single crystal, *Phys. Rev.* 82 (1951) 552.
- [16] H. Yamauchi, H. Hiroyoshi, M. Yamada, H. Watanabe, H. Takei, Spin flopping in MnTiO_3 , *J. Magn. Magn. Mater.* 31–34 (1983) 1071.
- [17] M. Wolf, K. Ruck, D. Eckert, G. Krabbes, K.-H. Müller, Spin-flop transition in the low-dimensional compound $\text{Ba}_2\text{Cu}_2\text{O}_4\text{Cl}_2$, *J. Magn. Magn. Mater.* 196–197 (1999) 569.
- [18] W. Zhang, K. Nadeem, H. Xiao, R. Yang, B. Xu, H. Yang, X.G. Qiu, Spin-flop transition and magnetic phase diagram in CaCoAs_2 revealed by torque measurements, *Phys. Rev. B* 92 (2015) 144416.
- [19] C.B. Liu, Z.Z. He, Y.J. Liu, R. Chen, M.M. Shi, H.P. Zhu, C. Dong, J.F. Wang, Magnetic anisotropy and spin-flop transition of NiWO_4 single crystals, *J. Magn. Magn. Mater.* 444 (2017) 190–192.
- [20] F.L.A. Machado, P.R.T. Ribeiro, J. Holanda, R.L. Rodriguez-Suarez, A. Azevedo, S.M. Rezende, Spin-flop transition in the easy-plane antiferromagnet nickel oxide, *Phys. Rev. B* 95 (2017) 104418.
- [21] G. Ghitgeatpong, M. Suewattana, S. Zhang, A. Miyake, M. Tokunaga, P. Chanlerit, N. Kurita, H. Tanaka, T.J. Sato, Y. Zhao, et al., High-field magnetization and magnetic phase diagram of $\alpha\text{-Cu}_2\text{V}_2\text{O}_7$, *Phys. Rev. B* 95 (2017) 245119.
- [22] X. Tan, V.O. Garlea, K. Kovnir, C.M. Thompson, T. Xu, H. Cao, P. Chai, Z.P. Tener, S. Yan, P. Xiong, et al., Complex magnetic phase diagram with multistep spin-flop transitions in $\text{L}_{0.25}\text{Pr}_{0.75}\text{Co}_2\text{P}_2$, *Phys. Rev. B* 95 (2017) 024428.
- [23] S.S. Samatham, S. Barua, K.G. Suresh, Spin-flop quasi-first order phase transition and putative tri-critical point in Gd_3Co , *J. Magn. Magn. Mater.* 444 (2017) 439.
- [24] B.R. Myoung, J.T. Lim, C.S. Kim, Investigation of magnetic properties on spin-ordering effects of FeGa_2S_4 and FeIn_2S_4 , *J. Magn. Magn. Mater.* 438 (2017) 121.
- [25] F.B. Anderson, H.B. Callen, Statistical mechanics and field-induced phase transitions of the heisenberg antiferromagnet, *Phys. Rev.* 136 (1964) 4A.
- [26] S. Blundell, *Magnetism in Condensed Matter*, Oxford University Press, Oxford, United Kingdom, 2003.
- [27] H.-F. Li, Possible ground states and parallel magnetic-field-driven phase transitions of collinear antiferromagnets, *Npj Comput. Mater.* 2 (2016) 16032.